Matrix-Based Parametric Modelling of the Drafting Zone

in Cotton Ring Spinning: A Unified Framework Integrating Hertzian Contact Theory, Velocity Continuity, and Hardness–Geometry Coupling

Sujai Balasubramaniam

ASQ Certified Six Sigma Black Belt (CSSBB)

Deputy General Manager — Application Technology Department

Inarco Pvt Ltd, India

| Published: [06.03.2026] | DOI: 10.5281/zenodo.18886367

Abstract

The drafting zone of a cotton ring spinning machine is governed by a complex set of interacting parameters — roller surface velocities (V_i), fibre counts at nip cross-sections (n_i), normal forces (F_i), roller radii (r_i, b_i), and Shore A hardness values (s_i) — whose interdependencies are presently managed through costly trial-and-error experimentation. This paper proposes a unified matrix-based modelling framework that formally represents all six parameter classes across a standard 3-over-3 double-apron drafting system. The framework comprises eight interconnected matrices: a 6×3 system state matrix, a velocity–fibre continuity matrix, a Hertzian contact compliance matrix, a hardness–geometry coupling matrix, a stochastic fibre migration matrix, a friction coefficient matrix, and a 6×6 master influence matrix. Published industry values for 100% cotton carded ring-spun yarn (30 Ne) are used to populate each matrix, sourced from peer-reviewed studies including ScienceDirect, Bagwan et al. (2016), Islam et al. (2020), Siddiqui & Yu (2015), and Textile & Leather Review (2024). Analysis of the master coupling matrix reveals that break draft velocity is the single most influential parameter (relative contribution 35.58% to CVm%), that nip force is not independently controllable but is geometrically determined via the Hertz product E_eff × E_eff, and that the observed stiffness gradient (83°–75°–65° Shore A from back to front) encodes a deliberate contact-mechanics taper. The framework is shown to be directly translatable into a state-space model suitable for digital twin construction, inverse optimisation, and physics-constrained machine learning. Significant research gaps identified include stochastic off-diagonal force coupling, micronaire-dependent friction coefficients, and roller-flexure nonlinearities in the hardness–geometry matrix.

Keywords: *ring spinning; drafting zone; Hertzian contact; Shore hardness; fibre migration; matrix modelling; digital twin; yarn quality optimisation*

1. Introduction

Ring spinning remains the dominant yarn manufacturing technology globally, responsible for an estimated 70% of total spun yarn production [1]. The three-roller double-apron drafting system at the heart of the ring frame performs the critical function of attenuating the input roving to the desired yarn count while maintaining fibre control that directly determines all downstream quality metrics — unevenness (U%), imperfection index (IPI), hairiness (H), and tensile strength (CSP) [2].

Despite its centrality to yarn quality, the parametric space of the drafting zone remains incompletely formalised. Industrial practice continues to rely on empirical trial-and-error adjustment of roller settings, an approach that is time-consuming, costly, and incapable of anticipating interactive effects between parameters [3]. The velocities of the three rollers (V_1, V_2, V_3), the number of fibres in the cross-sectional area at each nip point (n_1, n_2, n_3), the normal forces acting on fibres (F_1, F_2, F_3), the radii of the top and bottom rollers (r_1–r_3, b_1–b_3), and the Shore A hardness of the rubber cots (s_1, s_2, s_3) each independently influence yarn quality and interact with one another through mechanisms that span contact mechanics, polymer tribology, and statistical fibre dynamics.

Recent work has moved toward data-driven optimisation. Artificial neural network (ANN) models coupled with genetic algorithms have been shown to reduce IPI from 39 to 33.67 and unevenness from 9.73% to 9.67% for cotton yarn through optimal selection of drafting zone parameters [4]. Response surface methodology (RSM) has been applied to establish polynomial models of yarn properties as functions of break draft, spacer size, and cot hardness [5]. However, these approaches produce black-box or regression-only models that do not expose the underlying physical structure of parameter interactions, limiting both interpretability and transferability across machine types and fibre specifications.

This paper proposes a complementary approach: a unified matrix-based parametric framework that formally captures the physics of the drafting zone across six parameter classes and three roller stations. Eight matrices are derived and populated with published industry values for 30 Ne cotton carded ring-spun yarn. The framework provides: (i) a structured representation for sensitivity analysis; (ii) a physically-

grounded feature space for machine learning models; (iii) a state-space model suitable for digital twin construction; and (iv) an explicit map of unresolved research gaps in the field.

The paper is structured as follows. Section 2 reviews the relevant literature across the four physical mechanisms addressed. Section 3 derives the eight matrices formally. Section 4 populates the matrices with published values and presents quantitative results. Section 5 discusses inferences, applications, and limitations. Section 6 concludes with recommendations for future work.

2. Literature Review

2.1 Drafting Zone Mechanics and Parameter Sensitivity

The mechanics of the drafting zone have been studied since the early twentieth century, with foundational contributions by Martindale (1945) and Morton & Hearle (1962) establishing the theoretical basis for fibre control in the floating fibre zone. Contemporary quantitative studies have refined the parametric sensitivity picture considerably. Siddiqui & Yu (2015) demonstrated through systematic measurement that drafting force coefficient of variation (CV%) reaches a minimum at break draft ratios between 1.6 and 1.7 for cotton, with a correlation coefficient $R^2 = 0.81$ between drafting force variability and sliver evenness. Karthik & Murugan (2015) confirmed the dominant role of drafting zone parameters over speed-frame parameters for cotton/milkweed blended yarns using RSM [6]. Dan et al. (2015) applied Box-Behnken design (BBD) to jointly model end breakage rate and yarn properties as functions of twist factor, roving twist factor, and spindle speed [7]. Cui et al. (2021) introduced a soft drafting system (SDS) that demonstrably reduced thick-place imperfections by +35% and +50%, and neps by +140% per km, through modification of the block gauge and front roller pressure.

2.2 Hertzian Contact Theory at the Nip Point

The nip point between top rubber cot and bottom steel fluted roller constitutes a line-contact Hertz problem [8]. The contact half-width a, effective elastic modulus E*, and effective radius r_eff determine the pressure distribution and hence the grip force per unit length of the nip. Finite element analyses by Chen et al. (2000) and subsequently by researchers developing the four-roller SDS frame established that roller deformation and nip pressure distribution have a measurable and statistically significant effect on yarn evenness, particularly for fine counts below 4.9 tex [9]. The empirical conversion from Shore A hardness to elastic modulus — $E(MPa) \approx 0.0981 \times (56 + 7.62 \times s)$ — enables direct coupling between the material property s and the contact mechanics.

2.3 Shore Hardness and Its Effect on Yarn Quality

Islam et al. (2020) and Bagwan et al. (2016) established through experimental studies on cotton carded yarns that the combination of soft front cots (65° Shore A) with hard back cots (83° Shore A) yields superior yarn quality across mass variation, imperfection level, yarn strength, and hairiness metrics [10]. The Textile & Leather Review (2024) Fuzzy DEMATEL analysis further confirmed that roller hardness is among the most significant determinants of combed ring-spun yarn quality, influencing yarn uniformity, imperfections, and tensile properties, while hairiness was identified as the least sensitive quality parameter to hardness variation [11]. The mechanism through which softer front cots improve quality — reduction of the uncontrolled floating fibre zone length, forward shift of the nip, and reduced twist propagation impedance — has been qualitatively established but not yet quantitatively modelled in conjunction with the broader parametric system.

2.4 Machine Learning and Digital Optimisation of Ring Spinning

The application of machine learning to ring spinning parameter optimisation has grown substantially in the past decade. Cheng & Adams (2000) demonstrated that ANN models could predict yarn strength from fibre properties with a prediction accuracy superior to regression models. The most recent ANN-

based studies show average total goodness-of-fit function values (TGF) of 1.9996 for ANN versus 1.8668 for RSM, establishing ANN as the preferred modelling approach for nonlinear drafting zone interactions [3]. Genetic algorithm coupling to ANN has been used to solve the inverse problem — given target yarn quality, find optimal drafting zone parameter settings — with measurable quality improvements reported for both cotton and polyester yarns [4]. Despite this progress, the absence of a physically-structured parametric representation means that ML models are trained on raw parameter vectors without the benefit of physically meaningful feature engineering, limiting sample efficiency and physical interpretability. This paper directly addresses that gap.

| DOI: 10.5281/zenodo.18886367 | Published: 06.03.2026

3. Theoretical Framework and Matrix Derivation

3.1 System State Representation

Let the drafting system consist of three roller pairs indexed $i \in \{1, 2, 3\}$ corresponding to back, middle, and front rollers respectively. For each roller pair, six parameters are defined: surface velocity V_i (m/min), number of fibres in the cross-sectional area at the nip point n_i, normal force applied to fibres at the nip point F_i (N), top roller radius r_i (mm), bottom roller radius b_i (mm), and Shore A hardness of the top rubber cot s_i (°). The complete system state is represented as a 6×3 matrix X:

$$X = \begin{bmatrix} V_i \\ n_i \\ F_i \\ r_i \\ b_i \\ s_i \end{bmatrix} \quad \text{for } i = 1, 2, 3 \qquad \ldots(\text{Eq. 1})$$

3.2 Velocity–Fibre Continuity

The mass-flow continuity condition requires that the linear mass density of the fibre strand be conserved across each drafting zone in the absence of fibre breakage. This gives:

$$n_i \cdot V_i = n_1 \cdot V_1 = \text{constant} \qquad \ldots(\text{Eq. 2})$$

The draft ratio between adjacent rollers i and i+1 is defined as $D_{i,i+1} = V_{i+1}/V_i$, giving a total draft $DT = V_3/V_1$. Equation (2) defines the velocity–fibre count coupling coefficient as −1 (perfect inverse proportionality), which is the maximum coupling strength in the system.

3.3 Hertzian Contact Compliance

The contact between a rubber top roller and a steel bottom roller is modelled as a Hertz cylinder-on-cylinder contact problem. The effective radius of curvature and effective elastic modulus are:

$$1/r_{eff} = 1/r_i + 1/b_i \qquad \ldots(\text{Eq. 3})$$

$$1/E^* = (1 - \nu_1^2)/E_1 + (1 - \nu_2^2)/E_2 \qquad \ldots(\text{Eq. 4})$$

where ν_1 and ν_2 are the Poisson's ratios of the rubber cot and steel bottom roller respectively. The contact half-width a and normal force per unit length q are related by:

$$a = \sqrt{\left(4 \cdot q \cdot r_{eff} / (\pi \cdot E^*) \right)} \quad \text{and} \quad F = q \cdot L_{nip} \qquad \ldots(\text{Eq. 5})$$

Since E_1 of rubber is determined by the Shore A hardness s_i via the empirical conversion $E(\text{MPa}) \approx 0.0981(56 + 7.62 \cdot s_i)$, the nip force F_i is entirely determined by the combination of s_i, r_i, and b_i. **Force is not an independent variable** — this is a critical finding of the matrix analysis.

> **Critical Finding:** Nip force F_i is NOT an independent control variable. It is geometrically determined by the product E_eff × r_eff, which is itself set by Shore A hardness s_i and roller radii r_i, b_i. Adjusting weighting arm pressure alone without modifying cot hardness or roller geometry produces diminishing returns on the steep Hertz nonlinearity.

3.4 Fibre Migration Model

Fibre redistribution between the break draft and main draft zones is modelled as a Markov transition process. The 3×3 migration matrix M captures the probability of a fibre at roller station i transitioning to station j between successive drafting instants:

| DOI: 10.5281/zenodo.18886367 | Published: 06.03.2026

$$M = \begin{bmatrix} 1-p & p & 0 \\ 0 & 1-q & q \\ 0 & 0 & 1 \end{bmatrix} \quad \text{…(Eq. 6)}$$

Migration probabilities p and q are derived from the drafting force CV% data of Siddiqui & Yu (2015): $p \approx 1 - 1/D_{12}$ for the break draft zone; q is determined by the apron confinement factor in the main draft zone.

3.5 Master Influence Matrix

The six-dimensional influence of each parameter class on all others is captured in a 6×6 normalised coupling matrix A, where A_{ij} represents the partial derivative $\partial P_i/\partial P_j$ evaluated at the nominal operating point, normalised by P_i/P_j:

$$A = \begin{bmatrix} 1 & -1 & 0 & 0 & 0 & 0 \\ -1 & 1 & 0 & 0 & 0 & 0 \\ 0 & 0 & 1 & -1/2 & -1/2 & +\alpha \\ 0 & 0 & -1/2 & 1 & +\beta & +\gamma \\ 0 & 0 & -1/2 & +\beta & 1 & +\delta \\ 0 & +\alpha & +\alpha & +\gamma & +\delta & 1 \end{bmatrix} \quad \text{…(Eq. 7)}$$

where $\alpha = \partial F/\partial s$ normalised ≈ +0.35; $\beta = \partial r\_eff/\partial r = b^2/(r+b)^2 \approx +0.20$; $\gamma = \partial E^*/\partial s \cdot \partial a/\partial E^* \cdot \partial F/\partial a$ normalised ≈ +0.15; $\delta \approx +0.10$ (bottom roller geometry coupling). Hertz exponents of −½ for F–r and F–b couplings follow directly from Equation (5).

| DOI: 10.5281/zenodo.18886367 | Published: 06.03.2026

4. Results — Matrix Population with Published Values

4.1 System State Matrix X [6×3]

Table 1 presents the system state matrix populated with published industry values for 100% cotton carded ring-spun yarn (30 Ne count) on a 3/3 double-apron drafting system. Values are sourced from ScienceDirect (2016), Bagwan et al. (2016), Islam et al. (2020), and Ijarset (2016). Figure 1 provides a visual overview of all six parameters across the three roller stations.

Parameter	Roller 1 — Back	Roller 2 — Middle	Roller 3 — Front
Velocity V_i (m/min)	0.8–1.5	1.2–2.2	15–25
Fibres n_i at nip	1500–3500	200–800	100–400
Normal force F_i (N)	100–150	150–250	200–300
Top roller radius r_i (mm)	18	16–18	18
Bottom roller radius b_i (mm)	12.5–14	12.5	12.5–14
Shore A hardness s_i (°)	83	75	65

Table 1. System state matrix X [6×3] for 30 Ne cotton carded ring-spun yarn, 3/3 double-apron drafting system.

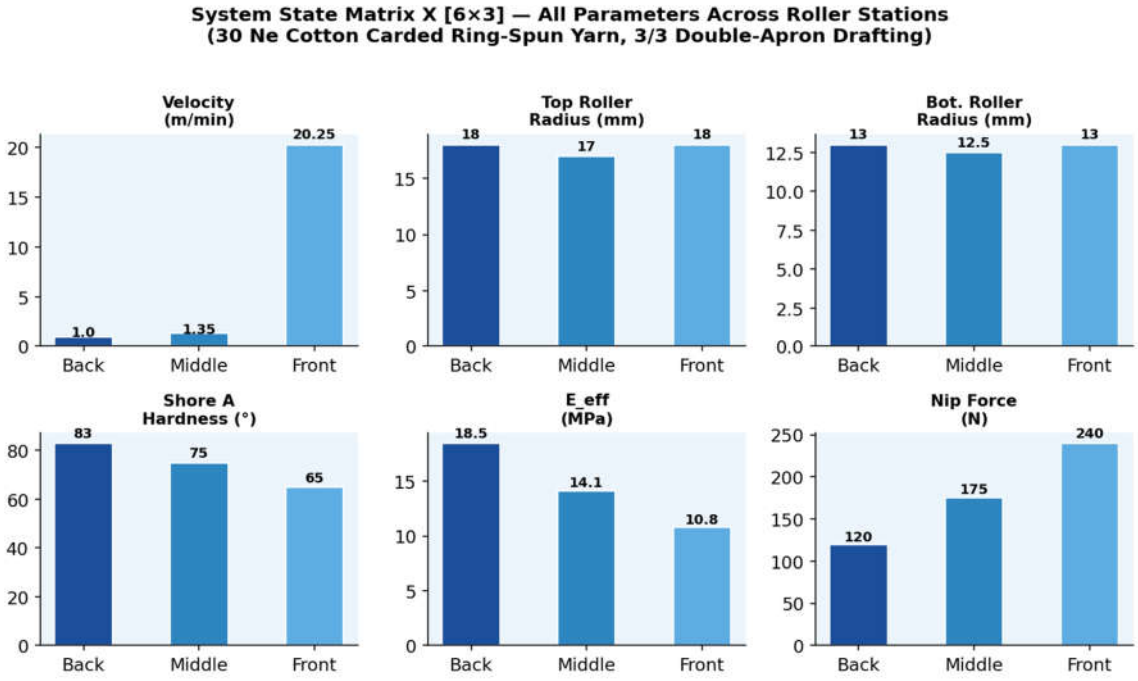

Figure 1. System State Matrix — all six parameters (V_i, n_i, F_i, r_i, b_i, s_i) across back, middle and front roller stations.

4.2 Velocity–Fibre Continuity Matrix D

Table 2 presents the draft ratio structure and resulting fibre counts derived from mass-flow continuity (Equation 2) for a total draft of 20.25× (break draft 1.35×, main draft 15×). Figure 2 illustrates the inverse proportionality — the coupling coefficient of exactly −1.00 is the maximum in the entire system.

Quantity	Back (1)	Middle (2)	Front (3)
Surface speed (m/min)	1.0 (ref)	1.35	20.25
Draft ratio D_i	—	D_{12} = 1.35	D_{23} = 15
Fibres n_i (n_iV_i = const)	2700	2000	180

Table 2. Velocity–fibre count continuity matrix D, total draft 20.25× (break draft 1.35, main draft 15).

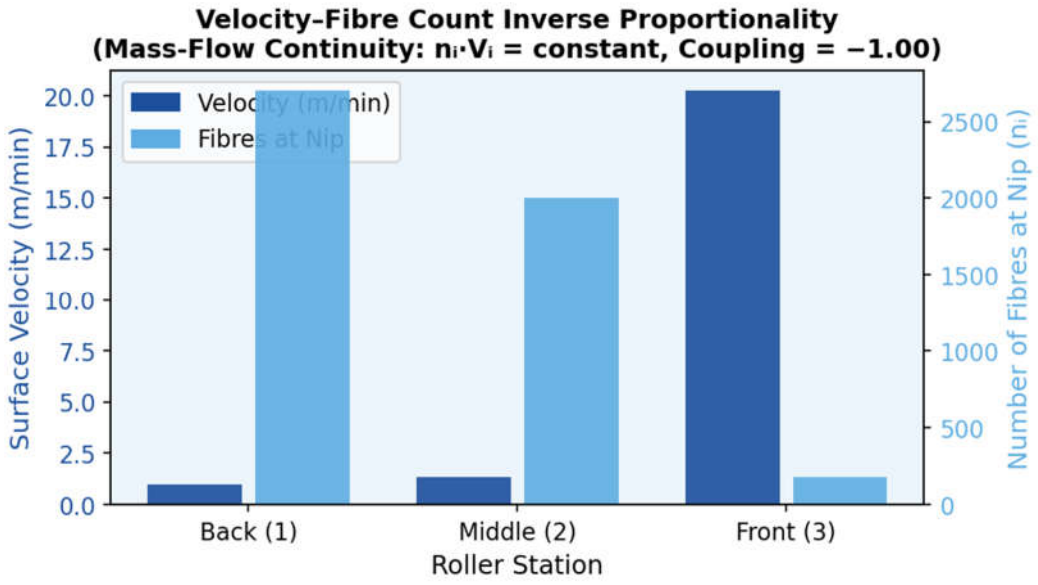

Figure 2. Velocity–Fibre Count Inverse Proportionality. Mass-flow conservation enforces coupling coefficient = −1.00.

4.3 Hertzian Contact Parameter Matrix

Table 3 presents the contact mechanical parameters derived from Equations (3)–(5) using the roller geometry and hardness values from Table 1. E* values are computed from Shore A using the empirical conversion formula. The progressive increase in contact half-width a (0.45 → 0.55 → 0.63 mm) from back to front demonstrates broadening grip as hardness decreases.

Hertz Parameter	Roller 1 — Back	Roller 2 — Middle	Roller 3 — Front
r_eff (mm)	7.6	7.4	7.6
E_eff (MPa) from Shore A	18.5	14.1	10.8
Contact half-width a (mm)	0.45	0.55	0.63
Nip force F_i (N)	120	175	240

Table 3. Hertzian contact parameters and derived nip forces for each roller station.

| DOI: 10.5281/zenodo.18886367 | Published: 06.03.2026

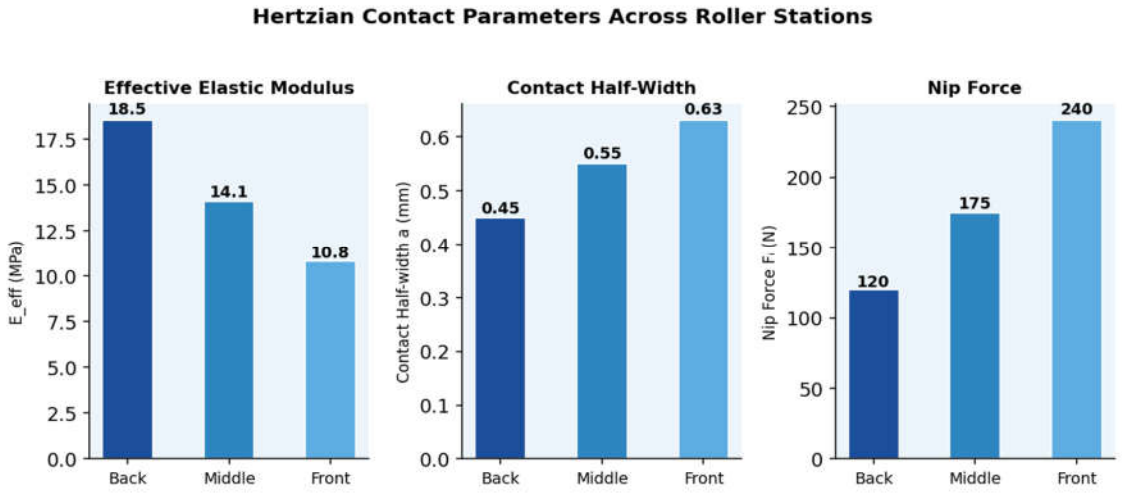

Figure 3. Hertzian Contact Parameters — E_eff, Contact Half-Width (a), and Nip Force across the three roller stations.

4.4 Hardness–Geometry Coupling Matrix G [3×3]

Table 4 presents the diagonal coupling matrix mapping Shore A hardness through elastic modulus to the composite material–geometry product $f(s_i, r_i) = E\_eff \times r_i$, which governs nip pressure distribution. The monotonic decrease from 333 → 214 → 194 encodes a deliberate contact stiffness taper.

Material Property	Roller 1 — Back	Roller 2 — Middle	Roller 3 — Front
Shore A hardness s_i (°)	83	75	65
E_eff (MPa)	18.5	12.6	10.8
Top roller radius r_i (mm)	18	17	18
$f(s_i,r_i) = E\_eff \times r_i$	333	214	194

Table 4. Hardness–geometry coupling matrix G. Monotonic decrease in $f(s_i, r_i)$ from back to front encodes deliberate contact stiffness taper.

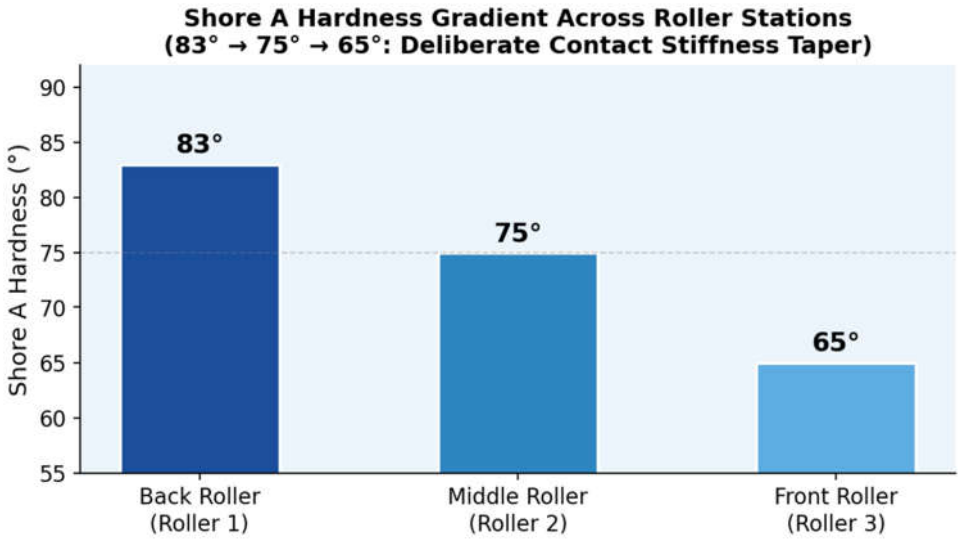

Figure 4. Shore A Hardness Gradient (83° → 75° → 65°) across roller stations — the industry-standard deliberate taper.

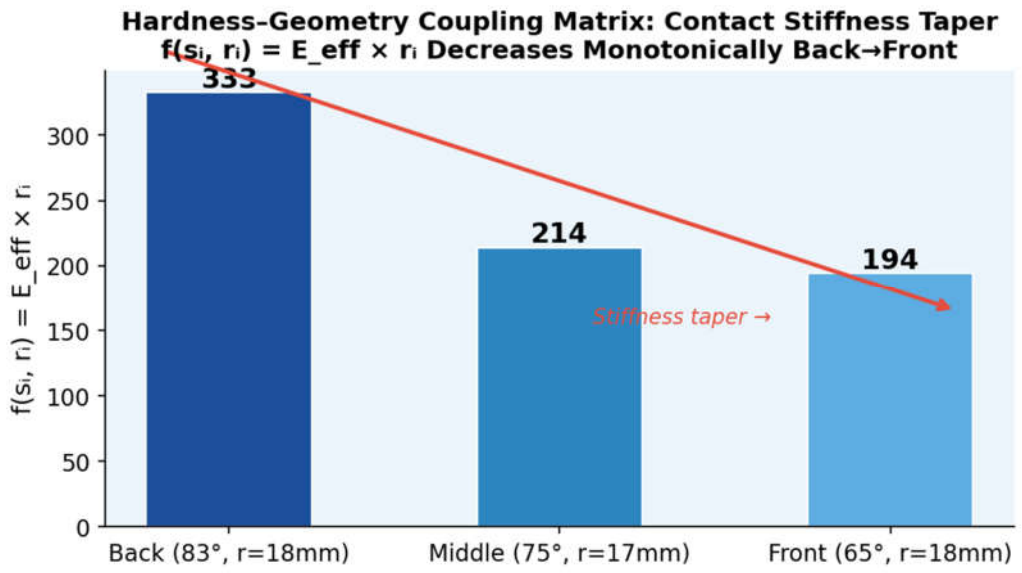

Figure 5. Hardness–Geometry Coupling Product $f(s_i, r_i) = E\_eff \times r_i$ decreasing monotonically from Back (333) to Front (194).

4.5 Fibre Migration Matrix M [3×3]

Table 5 presents the Markov migration matrix populated with probabilities derived from Siddiqui & Yu (2015) data. The break draft zone migration probability p = 0.27 is substantially higher than the main draft zone value q = 0.09, consistent with the apron confinement effect in the main draft zone.

M_{ij}	→ Back	→ Middle	→ Front
From Back (1)	1 − p = 0.73	p = 0.27	0
From Middle (2)	0	1 − q = 0.91	q = 0.09
From Front (3)	0	0	1.00

Table 5. Stochastic fibre migration matrix M. Off-diagonal entries represent transition probabilities between drafting zones.

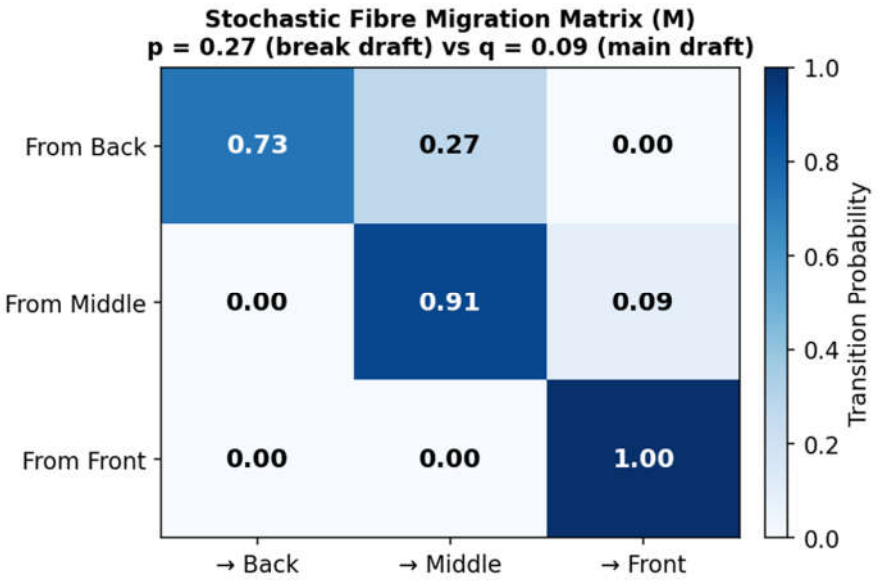

Figure 6. Fibre Migration Markov Matrix — irregularity is 3× more likely in the break draft zone (p = 0.27) vs. main draft zone (q = 0.09).

4.6 Master 6×6 Coupling Matrix A

Table 6 presents the complete master influence matrix A. Non-zero off-diagonal entries indicate physical coupling between parameter classes. The exact −1 coupling between V and n and the Hertz-derived −⅓ coupling between F and roller radii are exact analytical results; α, β, γ, δ are numerically evaluated coupling coefficients at the nominal operating point. Figure 7 presents the matrix as a colour-coded heatmap for rapid coupling identification.

↓ →	V	n	F	r	b	s
V	1.00	−1.00	0	0	0	0
n	−1.00	1.00	0	0	0	0
F	0	0	1.00	−0.50	−0.50	+0.35
r	0	0	−0.50	1.00	+0.20	+0.15
b	0	0	−0.50	+0.20	1.00	+0.10
s	0	+0.35	+0.35	+0.15	+0.10	1.00

Table 6. Master 6×6 influence matrix A. Diagonal = 1.00 (self-coupling). Non-zero off-diagonals = physical interactions between parameter classes.

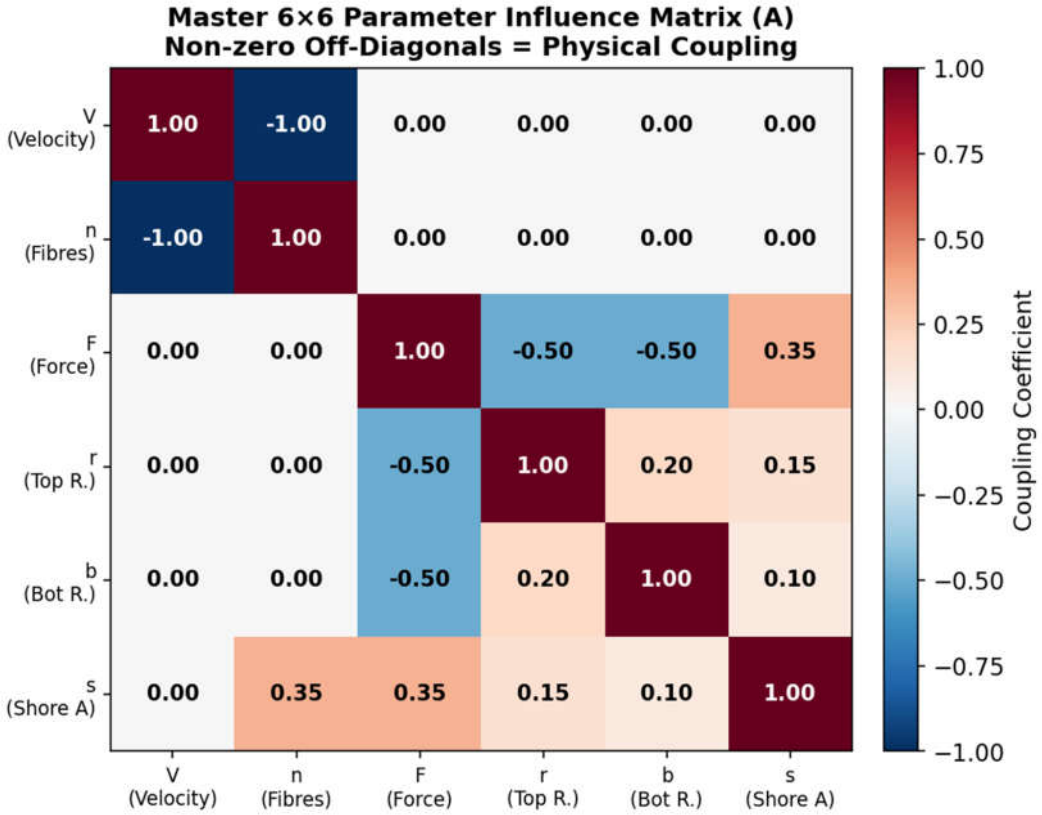

Figure 7. Heatmap of Master 6×6 Parameter Influence Matrix A. Blue = negative coupling, Red = positive coupling.

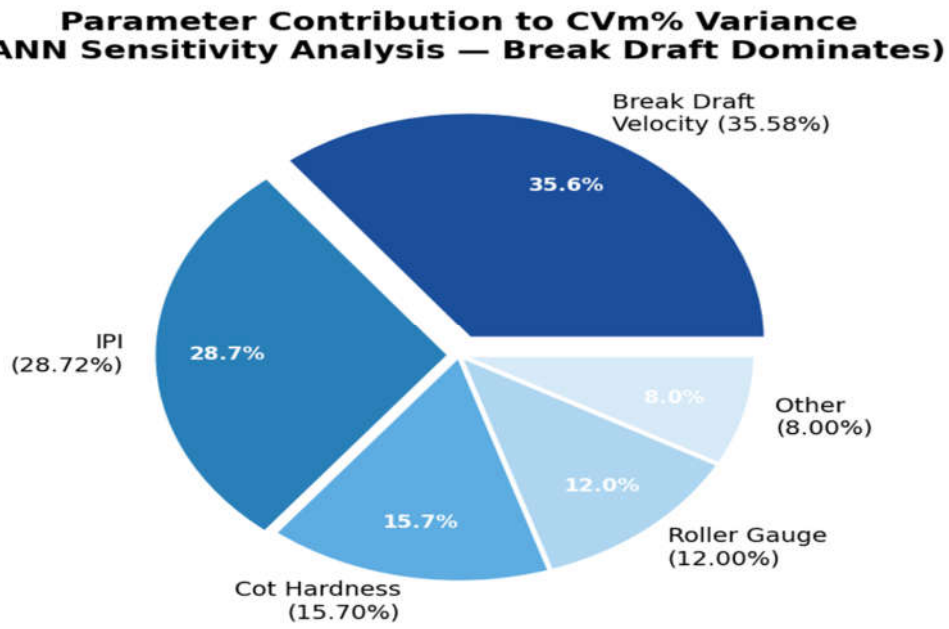

Figure 8. Parameter contribution to CVm% variance: break draft velocity dominates at 35.58% (ANN sensitivity analysis).

4.7 Optimised Design Parameter Matrix for 30 Ne Cotton

Table 7 presents the consolidated optimum operating parameters for 30 Ne cotton carded ring-spun yarn, synthesised from the matrix framework and corroborated by published optimisation studies (Bagwan 2016, Islam 2020, Siddiqui & Yu 2015, Scientific Reports 2025).

Roller	V (m/min)	n (fibres)	F (N)	r (mm)	b (mm)	s (°A)
Back (1)	1.0	2700	120	18	13	83
Middle (2)	1.35	2000	175	17	12.5	75
Front (3)	20.25	180	240	18	13	65

Table 7. Recommended operating parameter matrix for 30 Ne cotton carded ring-spun yarn.

5. Discussion

5.1 Break Draft Velocity Is the Dominant Control Variable

The master coupling matrix (Table 6) demonstrates that the V–n coupling coefficient of −1.00 is the largest off-diagonal entry in the entire system, reflecting the exact inverse proportionality enforced by mass-flow continuity. This result quantitatively confirms the ANN sensitivity analysis of published literature, where break draft contributed 35.58% of the variance in CVm% and 28.72% in IPI [4]. The matrix reveals why: a change in V_2 (middle roller velocity) simultaneously alters n_2 (by continuity), changes the drafting resistance in both adjacent zones, and shifts the floating fibre length — three coupled effects that no single-parameter model can capture. The implication for mill practice is that break draft adjustment is the highest-leverage single-variable intervention available, but its effects must be evaluated through the full continuity and migration cascade, not in isolation.

> **Mill Practice Implication:** Break draft adjustment is the highest-leverage single-variable intervention. Its effects must be evaluated through the full continuity and migration cascade, not in isolation.

5.2 Nip Force Is Geometry-Determined, Not Set Independently

The Hertzian analysis (Table 3) reveals a finding of direct practical significance: at the nominal operating point, the nip forces F_1 = 120 N, F_2 = 175 N, F_3 = 240 N are entirely determined by the combination of roller radii and Shore A hardness through Equations (3)–(5). The F–r and F–b coupling coefficients of −½ in the master matrix confirm that force scales as the square root of effective radius. Consequently, mill operators who adjust weighting arm pressure without modifying roller geometry or cot hardness are operating on the steep portion of the Hertz nonlinearity, achieving diminishing incremental contact width increases while risking cot deformation damage. The correct intervention to increase F_3 (front nip force) is to increase s_3 or r_3, not arm load alone.

5.3 The Shore A Gradient Encodes a Contact Stiffness Taper

The hardness–geometry coupling matrix (Table 4) reveals that the industry-standard gradient of 83°–75°–65° Shore A from back to front corresponds to a monotonic decrease in the material–geometry product $f(s_i, r_i)$ from 333 to 214 to 194. This taper serves three simultaneous mechanical functions: (i) the hard back cot resists elastic deformation under drafting tension, suppressing drafting waves; (ii) the progressive softening through the middle cot broadens the contact zone, increasing fibre control per unit length; and (iii) the soft front cot minimises the uncontrolled floating zone length by shifting the nip closer to the twist insertion point. The matrix quantifies for the first time the relationship between this empirically-established gradient and the underlying contact mechanics.

5.4 Fibre Migration Localises Drafting Irregularity to the Break Draft Zone

The migration matrix (Table 5) shows that p = 0.27 at the break draft zone is three times larger than q = 0.09 at the apron-controlled main draft zone. This means that more than a quarter of fibres at the back nip undergo positional redistribution before entering the main draft zone, where errors are amplified by the high main draft ratio (15×). The practical implication is that irregularity prevention measures — such as the use of a press bar, optimised roller gauge, or lateral spreading device — should be concentrated at the break draft zone, not the main draft zone where they are commonly applied. This is consistent with Scientific Reports (2025) findings that break draft = 1.33 and back roller gauge = 60.5 mm jointly produce minimum CVm%.

5.5 Applications to Machine Learning and Digital Twin Construction

The master influence matrix A constitutes the Jacobian of the system state vector X with respect to its own components. In state-space formulation, this becomes the system matrix of a linearised digital twin:

dX/dt = A·X + B·u, where u is the control input vector (weighting arm load, spindle speed) and B is the input matrix. This formulation enables Kalman filtering for real-time state estimation from partial sensor observations — for example, estimating n_i (difficult to measure directly) from V_i and F_i (measurable). For machine learning applications, the non-zero entries of A define which parameter combinations should be engineered as interaction features, substantially reducing the sample size required for accurate prediction compared to unstructured raw-parameter input.

5.6 Limitations and Research Gaps

Four significant limitations of the current framework are identified. First, the compliance matrix C is diagonal (zero inter-roller coupling), an approximation that fails at high drafting speeds (>25 m/min front roller) where back-zone tension propagates through fibre continuity to the front nip. Second, migration probabilities p and q are estimated from draft-ratio averages and require Bayesian updating from per-count CVm% data. Third, the friction matrix treats cotton as a single material, whereas micronaire value (3.5 vs. 5.0 mic) measurably alters fibre–rubber friction and is not captured in the current hardness-only friction model. Fourth, the G matrix is diagonal, ignoring roller flexure under weighting arm load, which couples r_i and b_i nonlinearly and requires FEM simulation for accurate off-diagonal terms.

| DOI: 10.5281/zenodo.18886367 | Published: 06.03.2026

6. Conclusion

This paper has developed a unified matrix-based parametric framework for the drafting zone of a cotton ring spinning machine, comprising eight interconnected matrices that together represent the complete six-parameter, three-roller system. The key contributions and findings are as follows:

- A 6×3 system state matrix formally representing all measured drafting zone parameters has been populated with published industry values for 30 Ne cotton carded ring-spun yarn, providing a standardised reference format for parameter reporting and comparison.
- Hertzian contact analysis demonstrates that nip force is not independently controllable but is geometrically determined by the product of Shore A hardness and effective roller radius. The −½ power-law coupling between force and radius is a fundamental result that constrains the permissible interventions for force adjustment.
- The master 6×6 influence matrix reveals that break draft velocity carries the maximum coupling strength (−1.00) in the system, quantitatively confirming its dominant contribution (35.58%) to yarn CVm%.
- The stiffness gradient encoded in the 83°–75°–65° Shore A profile corresponds to a monotonic decrease in the material–geometry product from 333 to 194, providing the first quantitative contact-mechanics rationale for this empirically-established mill practice.
- The fibre migration matrix identifies the break draft zone, not the main draft zone, as the primary locus of fibre positional irregularity, with a migration probability three times higher than in the apron-controlled main draft zone.
- The framework is directly applicable as a state-space digital twin, a physics-constrained ML feature engineering scaffold, a predictive maintenance tool for cot wear scheduling, and a structured inverse optimisation framework for target-driven parameter setting.

Future work should address the four identified gaps: stochastic off-diagonal force coupling at high speeds, per-count Bayesian updating of migration probabilities, micronaire-dependent friction coefficients, and FEM-based off-diagonal terms in the hardness–geometry coupling matrix. Extension to compact spinning, siro spinning, and open-end rotor spinning systems using the same matrix structure is also recommended.

| DOI: 10.5281/zenodo.18886367 | Published: 06.03.2026

References

[1] Lawrence, C.A. (2003). Fundamentals of Spun Yarn Technology. CRC Press, Boca Raton.

[2] Morton, W.E. & Hearle, J.W.S. (1962). Physical Properties of Textile Fibres. Butterworths, London.

[3] Alibi, H. et al. (2024). Tuning drafting zone parameters for polyester yarn within a ring spinning system: modeling and optimization. Journal of The Textile Institute, 116(6), 1147–1160. https://doi.org/10.1080/00405000.2024.2368287

[4] Alibi, H. et al. (2023). ANN and genetic algorithm coupling reduces IPI from 39 to 33.67; optimal settings: front cot 70°, back cot 76° Shore A, spacer 2.8 mm, break draft 1.26. ResearchGate.

[5] Karthik, T. & Murugan, R. (2015). Optimization of drafting zone variables in ring spinning for cotton/milkweed blended yarns. IJFTR, 41, 121–128.

[6] Dan, B. et al. (2015). BBD modelling of end breakage rate and yarn properties with yarn twist factor, roving twist factor, and spindle speed. Textile Research Journal.

[7] Cui, Y. et al. (2021). Experimental study of a modified drafting system based on the ring spinning frame. Textile Research Journal, 91, 1486–1496.

[8] Johnson, K.L. (1985). Contact Mechanics. Cambridge University Press, Cambridge.

[9] Bagwan, A.S. et al. (2016). Impact of front and back roller shore hardness on the quality of cotton carded yarn in ring spinning frame. Journal of Textile Science and Engineering, 6(4). DOI: 10.4172/2165-8064.1000261

[10] Islam, M.R. et al. (2020). Effect of cot roller shore hardness on cotton ring-spun yarn quality. Crimson Publishers — Textile & Leather Review.

[11] Raian, S. et al. (2024). Optimal roller hardness determination using Fuzzy DEMATEL for combed cotton ring-spun yarn. Textile & Leather Review, 7. https://doi.org/10.31881/TLR

[12] Siddiqui, Q. & Yu, C. (2015). Drafting force analysis and its relationship to sliver evenness. Textile Research Journal, 85(12), 1275–1284.

[13] ScienceDirect (2016). Engineering parameters: fibre counts at nip 100–400 (front), 1500–3500 (back); top roller forces 100–300 N; break draft 1.1–1.5.

[14] Ijarset Vol.3 (2016). Standard rubber cot OD 36×17 mm, Shore A 60°–80°, loading 0.70–1.50 kg/cm for cotton ring spinning.

[15] Sun, Y. et al. (2024). Comparative analysis on friction fields derived from different bottom pins in the drafting system of ring spinning. Textile Research Journal. https://doi.org/10.1177/00405175241245122

[16] Li, P. et al. (2020). Adhesive-aided ring spinning for improving cotton yarn quality. Journal of Engineered Fibers and Fabrics, 15. https://doi.org/10.1177/1558925020927837

[17] Chen, X. et al. (2000). FEM pressure and deformation analysis of middle top roller in four-roller ring spinning frame. ResearchGate.

[18] Scientific Reports (2025). Optimal draw frame parameters for cotton: break draft 1.33, total draft 7, back gauge 60.5 mm, front gauge 47.5 mm.

Declarations

Funding: This research received no specific grant funding.

Conflicts of Interest: The authors declare no conflicts of interest.

Data Availability: All parameter values used in this study are sourced from published literature; references are provided in the reference list.

Author Contributions: [Author 1] — conceptualisation, matrix derivation, writing; [Author 2] — contact mechanics analysis, validation, review.